RAPID COMMUNICATIONS

PHYSICAL REVIEW A VOLUME 44, NUMBER 10 15 NOVEMBER 1991

Diffusion-limited-aggregation model for Poisson growth

H. La Roche, J. F. Fernández, and M. Octavio
Instituto Venezolano de Investigaciones Científicas, Centro de Física, Apartado Postal 21827, Caracas 1020-A, Venezuela

A. G. Loeser and C. J. Lobb*
Division of Applied Sciences and Department of Physics, Harvard University, Cambridge, Massachusetts 02138
(Received 3 September 1991)

We propose an extension of the diffusion-limited-aggregation model for fractal growth. In our model, the Poisson equation is statistically simulated through the use of diffusive particles generated everywhere outside the aggregate. We relate the model to our experiments on viscous fingering in a Hele-Shaw cell in which flow is forced by separating the plates. Our simulations yield nonstationary fractal patterns which exhibit multiscaling and look much like the experimental patterns.

PACS number(s): 02.50.+s, 47.90.+a, 82.20.Wt

Diffusion-limited aggregation [1] (DLA) is the leading model of fractal growth [2–6]. It has been applied to a wide variety of phenomena: colloidal aggregation [1], viscous fingering [7,8], crystal growth [9], electrodeposition [10], and dielectric breakdown [11]. The common feature of these phenomena is that interfacial motion is controlled by Laplace's equation.

In the DLA model of the phenomena, diffusive particles are launched from a boundary far away from the aggregate. Each particle then executes a random walk until it lands on a site just outside the aggregate. The aggregate is then augmented by this selected site and the process is repeated for the next particle. Because the site-visitation probability is given by the solution of Laplace's equation, standard DLA (which we shall refer to as Laplace DLA) models stochastic growth governed by Laplace's equation.

In this Rapid Communication, we propose a generalized DLA model which corresponds, not to Laplace's equation, but to Poisson's equation. Particles are released one at a time not only from the boundaries but also from all points outside the aggregate with a probability that is proportional to the source term in Poisson's equation (see below). Laplace DLA can be thought of as a special case (often an approximation) of Poisson DLA. Viscous fingering into a *compressible* fluid, electrodeposition [12] when non-negligible ion generation occurs in an electrolytic solution, dielectric breakdown in a material with a charge distribution, and viscous fingering in a variable Hele-Shaw cell (which is the specific phenomenon we treat here), are all related to Poisson DLA. Poisson-DLA generated fractals (nonstationary in their fractal properties) are fundamentally different from Laplace DLA (approximately stationary [5]). This is because "fjords" are rather inaccessible to diffusive particles in Laplace DLA, but are easily visited in Poisson DLA by particles generated nearby. In this respect, our model is closer to other DLA-inspired nonstationary pattern-formation schemes of Voss [13] and Meakin [14] and the modified Ising model of Sørensen, Fogedby, and Mouritsen [15].

We illustrate Poisson DLA with an experiment: viscous fingering in a variable Hele-Shaw cell (VHSC) [16]. The glass plates which make up the cell are initially separated by grease of thickness h_0. Rather than displace the grease with injected air, one of the glass plates is lifted at one end using the opposite end as pivot. The grease then recedes towards the closed pivot end, drawing air (assumed to be inviscid) in at the open end (all other sides are sealed). This simple experiment is of practical interest: it is related to fracture properties of metallic glasses [17]. At the fracture plane, dilation-induced fluidization of the metallic glass in a thin layer provides the analog of the grease in the VHSC setup.

To compare the Poisson-DLA model to the VHSC experiment, we performed both experiments and the corresponding computer simulations that take into account surface tension [18]. A sequence of viscous fingers obtained experimentally and subsequently digitized is shown in Fig. 1(a). The corresponding set of viscous fingers given by the Poisson-DLA algorithm including surface tension is shown in Fig. 1(b). Their resemblance is striking. The features that distinguish Poisson DLA, however, are already present in the limit of vanishing surface tension. We will focus on this limit here.

To obtain Poisson's equation for the VHSC experiment, let $\mathbf{v}$, p, ρ, h, and μ, be the velocity, pressure, density, gap separation, and viscosity, respectively, at some point within the viscous fluid. Consider first the mass of fluid m within a thin column of height h perpendicular to the Hele-Shaw cell plates and let the plates separate ($\delta h/\delta t \neq 0$). Clearly, $\delta m/\delta t = \rho \delta h/\delta t$; it follows, therefore, from mass conservation, that

$$\frac{\partial h}{\partial t} = -h(\nabla \cdot \mathbf{v}) , \tag{1}$$

where $\mathbf{v}$ is now a two-dimensional vector

$$\nabla \cdot \mathbf{v} = \frac{\partial v_x}{\partial x} + \frac{\partial v_y}{\partial y} .$$

It follows then, taking the two-dimensional divergence of

the Poiseuille-Darcy equation [$\mathbf{v}=-(k/\mu)\nabla p$, where $k=h^2/12$], that

$$\nabla^2 p=\frac{\mu}{k}\left[\frac{1}{h}\frac{\partial h}{\partial t}\right], \tag{2}$$

which is Poisson's equation. In deriving Eq. (2), we have used $\nabla h \approx 0$ for nearly parallel plates.

To describe the Poisson-DLA model, consider a cell of $L\times L$ sites. We use periodic boundary conditions for both the left and the right sides. The aggregate grows towards the top. The interface-boundary (IB) sites are nearest neighbors to the aggregate sites. We call sites exterior to the aggregate, but not part of IB, exterior sites (ES). Boundary conditions for a field ϕ are $\phi=g(\mathbf{x})$ on the aggregate and $\partial\phi/\partial n=0$ at the top of the cell (for a VHSC cell sealed at the top). Each site i in ES and k in IB has values $f_i=f(\mathbf{x}_1)$ and $g_k=g(\mathbf{x}_k)$ associated with it, where f is the source term in a Poisson equation $\nabla^2\phi=f$ [see, for example, Eq. (2)]. We deal here with $f,g>0$, only.

We next show that a modified DLA model can be used to simulate Eq. (2). Diffusive particles are generated one at a time anywhere outside of the aggregate (in ES or IB) and vanish upon aggregation. To show that the probability for a particle to originate at i in ES is f_i or at k at IB is g_s, we roughly follow Kadanoff's [8] scheme. Suppose we start off N diffusive particles, Nf_i of them at each site i in ES and Ng_l at each site l in IB. We assume $\sum f_i+\sum g_k=1$. Each of the walkers hops to a nearest-neighbor site with equal probability each time step. All particles vanish when they reach an IB site and bounce off the cell top boundary (since $\partial\phi/\partial n=0$). The process stops when the particles have vanished. Clearly,

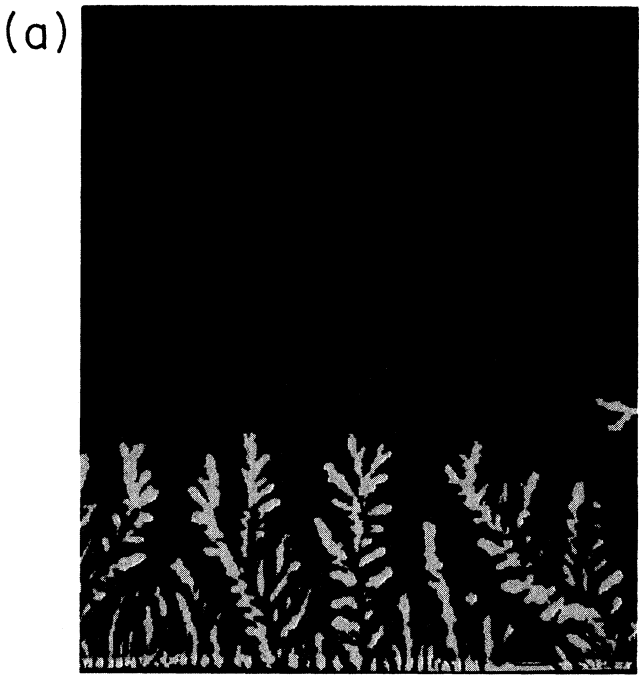

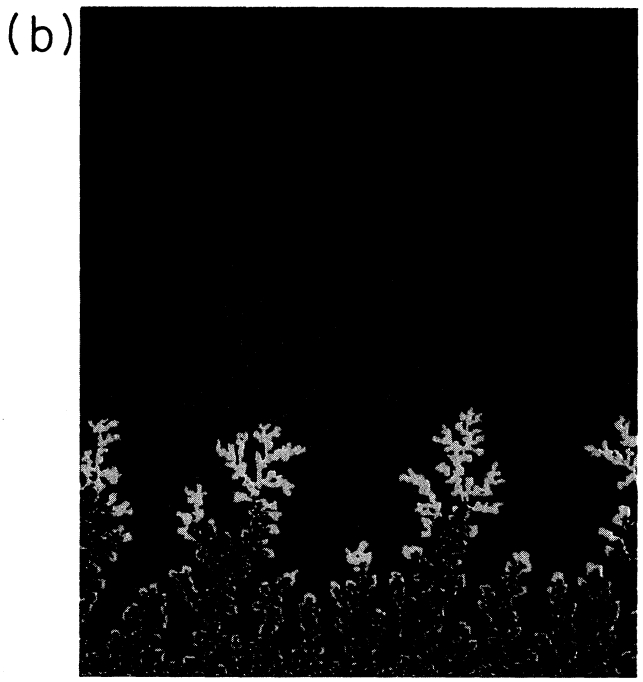

FIG. 1. Digitized images from (a) the separating plates experiment and (b) associated computer simulation. Plate dimensions in (a) are approximately 9 cm×9 cm, initial separation between the plates is 0.05 mm. The rate of separation at the lifted end is 0.025 cm/min.

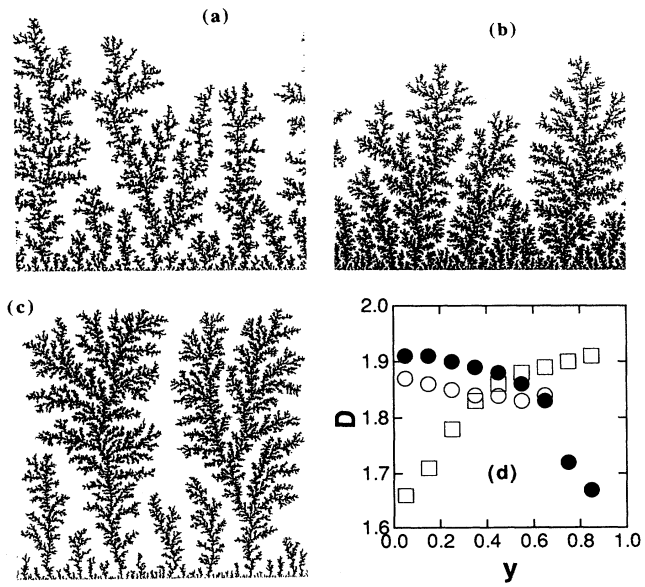

FIG. 2 Aggregates obtained from simulations and their Hausdorff dimension. In (a), the source is constant. Case (b) corresponds to a source $f\propto L-y$. In (c), $f\propto y$. (d) shows the Hausdorff dimension profile on horizontal strips along the y axis for aggregates of size 30% of cell size (1024×1024). Strips are of width 128 sited and correspond to the three aggregates shown with ○ corresponding to (a), ● corresponding to (b), and □ corresponding to (c).

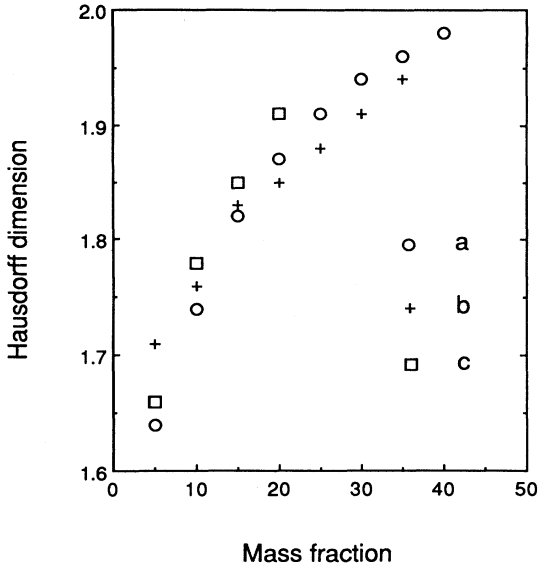

FIG. 3. Fractal dimension vs aggregate size (expressed as a ratio of the number of sites to lattice size). Cell size is 1024×1024. Data for aggregates that have reached the top are not plotted.

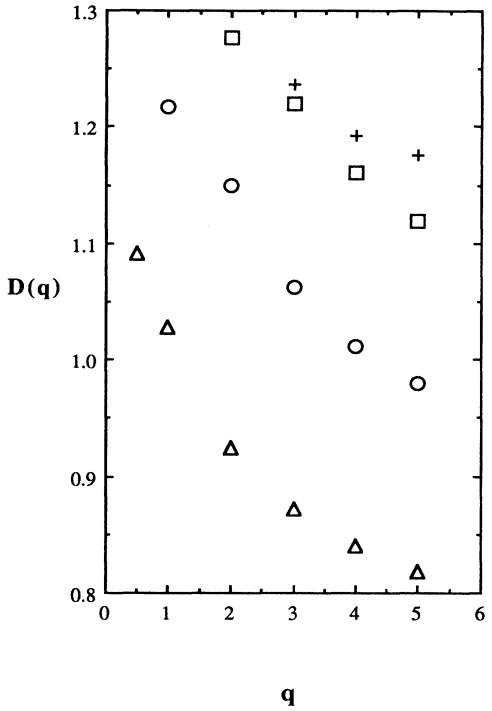

FIG. 4. The generalized dimension $D(q)$ for different mass ratios m. The symbols △, ○, □, and + represent 1%, 5%, 10%, and 30% mass ratios.

$$N_i^{t+1}=\tfrac{1}{4}\sum_{j\in\langle i\rangle} N_j^t\ , \tag{3}$$

where $\langle i\rangle$ stands for the set of nearest-neighbor sites to i, and N_i^t stands for the number of particles at i at time t. For a site k in ES, $N_k^{t+1}=N_k^t\delta_{0,t}=Ng_k\delta_{0,t}$. Subtract N_i^t from both sides of Eq. (3) and sum over t from $t=0$ to the time when all particles have vanished (say $t\to\infty$), to obtain

$$-N_i^0=\tfrac{1}{4}\sum_{j\in\langle i\rangle}\left[\sum_{t=0}^{\infty}N_j^t-\sum_{t=0}^{\infty}N_i^t\right] \tag{4}$$

for any i in ES. Therefore the average number of times that a particle visits a site i, $(1/N)\sum_{t=0}^{\infty}N_i^t$, obeys Poisson's equation on sites i in ES and is g_k for k in IB, and can thus be identified with ϕ demonstrating the statistical validity of the algorithm.

We performed simulations using three different source terms on lattices of up to 1024×1024. Figure 2(a) shows an aggregate grown with a constant source term. Figure 2(b) shows the same for a source that varies linearly from zero at the bottom of the cell to unity at the top. In Fig. 2(c), the source is zero at the top and increases to unity at the bottom. This last case is like the experimental case without the surface tension. For these simulations, we have calculated a profile of the fractal dimensionality along the y axis, $D(y)$, by using horizontal strips wide enough (in terms of cells of the lattice) for good fractal statistics, and yet as thin as possible. Calculating the Hausdorff dimension for all the lattice cells in the strip gives some "average" fractal dimensions at a given y value. These results are exhibited in Fig. 2(d) [19]. Clearly, the local fractal dimensionality reflects the strength of the source term. Figure 3 displays the evolution of the Hausdorff dimension $D_{\rm H}$ [which can be shown to be the maximum value of $D(y)$]. As the aggregate gradually fills all the cell space, we find the $D_H\to2$.

The dynamics of Poisson DLA, as for Laplace DLA, is given by the growth measure [3,20-22]. We focus on the ensemble of aggregates grown in a lattice of $L\times L$ sites, $\Omega_m(L)$, where $m=M/L^2$ and M is the number of particles in the aggregate [23]. The parameter m (mass fraction) may be thought of as a sort of time. The growth measure for an aggregate ω in $\Omega_m(L)$ is given in terms of the set $\{P_k(\omega)\}_{k\in\rm IB}$ of growth probabilities which is obtained following Refs. [20] and [21]: an aggregate is grown to mass fraction m at which point launchings of random walkers continue but aggregations stop. Then $P_k=\lim_{N\to\infty}N_k/N$ where N_k is the number of walkers that vanished at site k.

To find out if $\{P_k(\omega)\}_{k\in\rm IB}$ is a multifractal measure [24] on IB, we calculate, for various ω in $\Omega_m(L)$,

$$\zeta(q;m,L)=\sum_{i\in\rm IB}P_i^q \tag{5}$$

and test the scaling behavior assumption $\zeta\sim L^{-(q-1)D(q)}$ (for a source of the form $f\propto L-y$). Our results, which are shown in Fig. 4, are consistent with this scaling assumption [25]. There is no unique scaling exponent for all m [$D(q)$ depends on m]. For small m, when the aggregate lies within a region where the source is weak, the curve coincides with the Laplace-DLA curve (reported in Refs. [20] and [21]) as expected. As m grows and the aggregate penetrates regions where the source effects be-

come significant, the shape of $D(q)$ changes dramatically.

The authors would like to thank K. Octavio, J. Aponte, J. M. Albarrán, A. Leon, and A. Shiekh for help with image analysis, and G. Mendoza, D. Weitz, F. Spaepen, and L. E. Guerrero for useful conversations. This work was supported in part by NSF Grant No. DMR-89-20490.

---

*Present address: Department of Physics, Center for Superconductivity Research, University of Maryland, College Park, MD 20742.

[1] T. A. Witten and L. M. Sander, Phys. Rev. Lett. **47**, 1400 (1981); Phys. Rev. B **27**, 5686 (1983).

[2] *On Growth and Form,* edited by H. E. Stanley and N. Ostrowsky (Martinus Nijhoff, Dordrecht, 1985).

[3] *Random Fluctuations and Pattern Growth,* edited by H. E. Stanley and N. Ostrowsky (Kluwer Academic, Dordrecht, 1988).

[4] *Kinetics of Aggregation and Gelation,* edited by F. Family and D. P. Landau (North-Holland, Amsterdam, 1984).

[5] J. Feder, *Fractals* (Plenum, New York, 1988).

[6] T. Vicsek, *Fractal Growth Phenomena* (World Scientific, Singapore, 1989).

[7] L. M. Paterson, Phys. Rev. Lett. **52**, 1621 (1984).

[8] L. P. Kadanoff, J. Stat. Phys. **39**, 267 (1985).

[9] H. Honjo, S. Ohta, and M. Matsushita, J. Phys. Soc. Jpn. **55**, 2487 (1986).

[10] R. M. Brady and R. C. Ball, Nature (London) **309**, 225 (1984); M. Matsushita, M. Sano, Y. Hayakawa, H. Honjo, and Y. Sawada, Phys. Rev. Lett. **53**, 286 (1984).

[11] L. Niemeyer, L. Pietronero, and H. J. Wiesmann, Phys. Rev. Lett. **52**, 1083 (1984); L. Peitronero and H. J. Wiesmann, J. Stat. Phys. **36**, 909 (1984).

[12] J. R. Melrose, D. B. Hibbert, and R. C. Ball, Phys. Rev. Lett. **65**, 3009 (1990).

[13] R. F. Voss, Phys. Rev. B **30**, 334 (1984); J. Stat. Phys. **36**, 861 (1984).

[14] P. Meakin, Phys. Rev. A **26**, 1495 (1983); **27**, 2616 (1983); see also P. Meakin, in *Phase Transitions and Critical Phenomena,* edited by C. Domb and J. L. Lebowitz (Academic, New York, 1988), Vol. 12, p. 336.

[15] E. S. Sørensen, H. C. Fogedby, and O. Mouritsen, Phys. Rev. A **39**, 2194 (1989).

[16] VHSC experiments have been reported in the past, but no relation to Poisson DLA was given; see E. Ben-Jacob, R. Godbey, N. D. Goldenfeld, J. Koplik, H. Levine, T. Mueller, and L. M. Sander, Phys. Rev. Lett. **55**, 1315 (1985).

[17] C. A. Pampillo and A. C. Reimschuessel, J. Mater. Sci. **9**, 718 (1974); F. Spaepen and D. Turnbull, Scr. Metall, **8**, 563 (1974); F. Spaepen, Acta Metall. **23**, 615 (1975).

[18] We incorporate surface-tension effects in the Poisson-DLA model following J. F. Fernández and J. M. Albarrán, Phys. Rev. Lett. **64**, 2133 (1990). Details concerning the experiments and simulations incorporating surface tension will be given elsewhere.

[19] It would be preferable to define fractal dimension $D(\mathbf{x})$ at every point $\mathbf{x}$ instead of averaging over the width to obtain $D(y)$. Unfortunately, there are not enough points in our simulated aggregates to measure $D(\mathbf{x})$ in sufficiently small disks around each point in the aggregate.

[20] T. C. Halsey, P. Meakin, and I. Proccacia, Phys. Rev. Lett. **56**, 854 (1986).

[21] C. Amitrano, A. Coniglio, and F. di Liberto, Phys. Rev. Lett. **57**, 1016 (1986).

[22] B. B. Mandelbrot and C. J. G. Evertsz, Nature (London) **348**, 143 (1990).

[23] For Laplace DLA, which is sometimes assumed to be self-similar, the full ensemble of aggregates (no size restriction) is considered. See J. Lee and H. E. Stanley, Phys. Rev. Lett. **61**, 2945 (1988); Phys. Rev. A **39**, 6545 (1989).

[24] H. G. E. Hentschel and I. Procaccia, Physica D **8**, 435 (1983); T. C. Halsey, M. H. Jensen, L. P. Kadanoff, I. Procaccia, and B. I. Shraiman, Phys. Rev. A **33**, 1141 (1986).

[25] Multifractality crucially depends on the validity of the scaling hypothesis. For an analysis of this issue in the context of Laplace DLA, see R. Blumenfeld and A. Aharony, Phys. Rev. Lett. **62**, 2977 (1989).

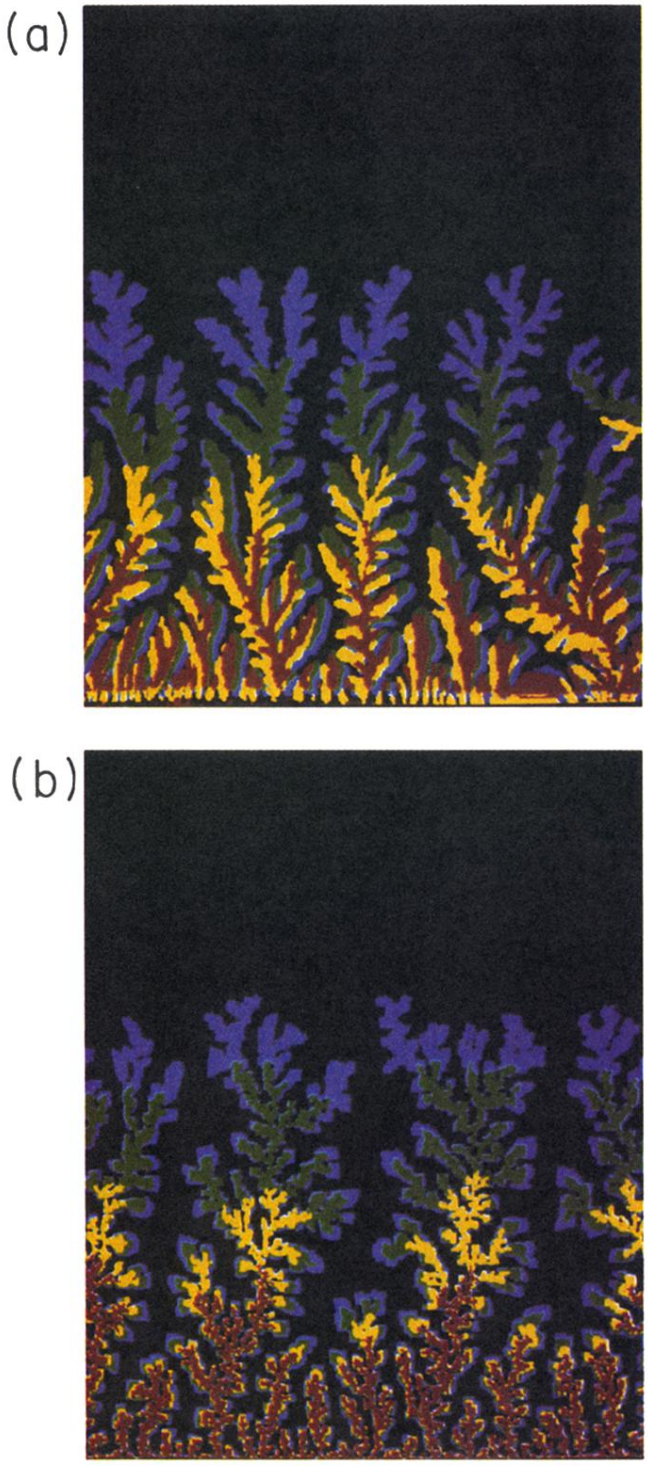

FIG. 1. Digitized images from (a) the separating plates experiment and (b) associated computer simulation. Plate dimensions in (a) are approximately 9 cm×9 cm, initial separation between the plates is 0.05 mm. The rate of separation at the lifted end is 0.025 cm/min.